



Published in final edited form as:

Int J Radiat Oncol Biol Phys. 2008 January 1; 70(1): 2–13. doi:10.1016/j.ijrobp.2007.06.039.

Fluorine-18-Labeled Fluoromisonidazole Positron Emission and Computed Tomography-Guided Intensity-Modulated Radiotherapy for Head and Neck Cancer: A Feasibility Study

Nancy Y. Lee, M.D.^{*}, James G. Mechalakos, Ph.D.[†], Sadek Nehmeh, Ph.D.[†], Zhixiong Lin, M.D.[†], Olivia D. Squire, R.N.[‡], Shangde Cai, Ph.D.[‡], Kelvin Chan, B.A.^{*}, Pasquale B. Zanzonico, Ph.D.[†], Carlo Greco, M.D.^{*}, Clifton C. Ling, Ph.D.[†], John L. Humm, Ph.D.[†], and Heiko Schöder, M.D.[‡]

^{*}Department of Radiation Oncology, Division of Nuclear Medicine, Memorial Sloan-Kettering Cancer Center, New York, NY

[†]Department of Medical Physics, Division of Nuclear Medicine, Memorial Sloan-Kettering Cancer Center, New York, NY

[‡]Department of Radiology, Division of Nuclear Medicine, Memorial Sloan-Kettering Cancer Center, New York, NY

Abstract

Purpose—Hypoxia renders tumor cells radioresistant, limiting locoregional control from radiotherapy (RT). Intensity-modulated RT (IMRT) allows for targeting of the gross tumor volume (GTV) and can potentially deliver a greater dose to hypoxic subvolumes (GTV_h) while sparing normal tissues. A Monte Carlo model has shown that boosting the GTV_h increases the tumor control probability. This study examined the feasibility of fluorine-18-labeled fluoromisonidazole positron emission tomography/computed tomography (¹⁸F-FMISO PET/CT)-guided IMRT with the goal of maximally escalating the dose to radioresistant hypoxic zones in a cohort of head and neck cancer (HNC) patients.

Methods and Materials—¹⁸F-FMISO was administered intravenously for PET imaging. The CT simulation, fluorodeoxyglucose PET/CT, and ¹⁸F-FMISO PET/CT scans were co-registered using the same immobilization methods. The tumor boundaries were defined by clinical examination and available imaging studies, including fluorodeoxyglucose PET/CT. Regions of elevated ¹⁸F-FMISO uptake within the fluorodeoxyglucose PET/CT GTV were targeted for an IMRT boost. Additional targets and/or normal structures were contoured or transferred to treatment planning to generate ¹⁸F-FMISO PET/CT-guided IMRT plans.

Results—The heterogeneous distribution of ¹⁸F-FMISO within the GTV demonstrated variable levels of hypoxia within the tumor. Plans directed at performing ¹⁸F-FMISO PET/CT-guided IMRT for 10 HNC patients achieved 84 Gy to the GTV_h and 70 Gy to the GTV, without exceeding the normal tissue tolerance. We also attempted to deliver 105 Gy to the GTV_h for 2 patients and were successful in 1, with normal tissue sparing.

Reprint requests to: Nancy Y. Lee, M.D., Department of Radiation Oncology, Memorial Sloan-Kettering Cancer Center, 1275 York Ave., New York, NY 10021. Tel: (212) 639-3341; Fax: (212) 639-2417; leen2@mskcc.org.

Zhixiong Lin, M.D. is currently at the Cancer Hospital-Shantou University Medical College, People's Republic of China.

Presented at the Forty Seventh Annual Meeting of the American Society for Therapeutic Radiology and Oncology (ASTRO), Denver, CO, October 13–16, 2005.

Conflict of interest: none.

Conclusion—It was feasible to dose escalate the GTV_h to 84 Gy in all 10 patients and in 1 patient to 105 Gy without exceeding the normal tissue tolerance. This information has provided important data for subsequent hypoxia-guided IMRT trials with the goal of further improving locoregional control in HNC patients.

Keywords

Intensity-modulated radiotherapy; Hypoxia; Fluorine-18-labeled fluoromisonidazole; ¹⁸F-FMISO; Positron emission tomography

Introduction

Hypoxia is a characteristic feature of malignant tumors (1–4). The distribution of hypoxic cells has been shown at the microscopic level using immunohistochemical methods. These studies have suggested that hypoxia exists as nests or bands of cells ranging from a few micrometers up to several hundred micrometers in diameter (5,6). Hypoxia can render tumor cells up to three times more resistant to radiation relative to aerobic cells (7). Hypoxia has been shown in several studies to be an important determinant of locoregional control (LRC) and overall survival in many tumors, including head and neck cancer (HNC) (2,8–13).

Although direct measurements of tumor hypoxia using the Eppendorf electrode have been considered a reference standard for measuring hypoxia, it is difficult to perform sufficient measurements at defined accurate locations to render the information useful for treatment planning. Furthermore, its use requires a skilled operator, and it is invasive, subject to sampling errors, and unable to exclude low readings obtained from nonviable necrotic tissue (2,4,12–17). Other methods have claimed equivalent accuracy (*e.g.*, the Comet assay) (18). However, the Comet assay, along with immunohistochemical approaches of staining endogenous or exogenous markers (19,20) suffer from sampling errors because of the ability to only analyze limited sectional information derived from attainable biopsy samples.

Investigators have sought to use a noninvasive imaging method that could provide a spatial map of the hypoxia distribution relative to the body anatomy and be readily incorporated in radiotherapy (RT) planning. The current widespread deployment of positron emission tomography/computed tomography (PET/CT) units has allowed such a possibility if suitable PET tracers (currently under investigation) (16,21,22) that selectively localize in tumor hypoxia, can be identified. PET imaging using hypoxia tracer fluorine-18-labeled fluoromisonidazole (¹⁸F-FMISO) has been extensively studied in several cancers at the University of Washington (23–27). This fluorinated radiotracer was developed out of extensive earlier investigation of the parent nitroimidazole compound misonidazole, which had been developed as a hypoxic cell radiosensitizer, in the 1970–1980s (28). Rasey *et al.* (29) have demonstrated the efficacy of PET imaging with ¹⁸F-FMISO in quantifying hypoxia in HNC patients and observed a marked variability and heterogeneity between tumors in the same site or of the same histologic type.

A Monte Carlo model developed by Popple *et al.* (30) studied the effects on tumor control probability from hypoxia by selectively boosting the radiation dose to the hypoxic subvolume within the gross tumor volume (GTV), namely, the GTV_h. The investigators divided each tumor into two compartments such that portions of the tumor received a primary tumoricidal dose and other portions received a higher tumor dose. In addition, different clonogenic subpopulations were also defined: those that were well oxygenated; those with transient hypoxia; and those with chronic hypoxia. The effects of reoxygenation were also included in this model. The investigators concluded that an increase of 120–150% of the primary tumor dose can increase the tumor control probability equivalent to that of tumors without chronic

hypoxia. They further found that it was not necessary to dose escalate the entire hypoxic subvolume to obtain a significant increase in the tumor control probability (30).

Recent studies have shown excellent treatment outcomes, in particular, reduced rates of xerostomia in HNC patients treated with IMRT (31–33). Investigators have also shown that in these patients, tumor recurrence tends to occur within the GTV (34–36). This could be attributed to the more radioresistant GTV_h within the GTV. One could dose escalate the entire GTV; however, an indiscriminate increase in the dose to the GTV could deliver unnecessary radiation to the normal tissues found within or around the GTV, possibly at the expense of increasing the incidence of late complications. An alternative method is to differentially dose escalate within the GTV (37–41). Because IMRT has the ability to dose paint different regions within the target, one can use this technology to selectively deliver an increased dose to the GTV_h if the intratumor location can be identified. In this study, we used ^{18}F -FMISO PET to provide a spatial map of the intratumor distribution of tumor hypoxia and, thus, identification of the GTV_h . This would allow IMRT plans to be generated for the GTV, with a supplemental dose to the GTV_h , while limiting the radiation dose delivered to the normal tissues (42). Chao *et al.* (21) demonstrated the feasibility of this approach for 1 HNC patient using Cu(II)-diacetyl-bis(N4-methylthiosemicarbazone) (Cu-ATSM) as a hypoxia tracer to perform hypoxia dose painting IMRT.

In this report, we sought to demonstrate the feasibility of dose escalation using hypoxia-guided dose-painting IMRT by incorporating the hypoxia uptake information obtained from ^{18}F -FMISO PET in a cohort of HNC patients. The ultimate goal was to increase LRC of HNC by the delivery of a differential radiation dose to the GTV, along with its GTV_h , while not delivering excessive radiation to the surrounding normal tissues.

Methods and Materials

Patient characteristics

A prospective Memorial Sloan-Kettering Cancer Center trial titled “A Feasibility Study of Using Fluorine-18–Labeled Fluoromisonidazole Positron Emission Tomography to Detect Hypoxia in Head-and-Neck Cancer Patients” was opened to patient accrual in 2004 (institutional review board No. 04-070). A total of 28 patients provided written informed consent and were enrolled between August 2004 and October 2005. Of these 28 patients, 20 underwent fluorodeoxyglucose (FDG) PET and three subsequent ^{18}F -FMISO scans, for a total of four PET scans, without any problems, and 8 subsequently decided not to participate in the study: 1 because of claustrophobia and 7 because of personal life choices (*i.e.*, concerns regarding the number of additional hospital visits or additional number of scans). The patients were all men, with a median age of 60 years. Of the 20 patients who underwent scanning, 8 were excluded from the present study because of a missing blood profile for 6 or coagulated blood for 2. Since these exclusions, our multidisciplinary team has met to ensure that subsequent patients who participate in this feasibility study all have full blood profiles and that care was taken to ensure that the blood was not coagulated. Significant ^{18}F -FMISO uptake has been reported by Rajendran *et al.* (23,42–44) to be at tumor/blood (T/B) ratio of 1.2–1.4. In the absence of a reference standard threshold value to define hypoxia, our desire was to select a single threshold value for demarcation of the GTV_h to conform to uniform planning parameters. To this end, we selected an intermediate threshold value from the range quoted by Rajendran *et al.* of 1.3. This led to the additional exclusion of 2 patients, for whom it was noted that a 1.3 T/B threshold resulted in almost complete GTV coverage and for whom significantly greater T/B ratios were observed. Because of our desire not to use patient-specific T/B thresholds to minimize any additional subjectivity that might affect the results of our IMRT planning, only 10 patients were included in the present feasibility study of ^{18}F -FMISO PET/CT-guided IMRT. Although hypoxia-based IMRT plans were generated for 10 patients, these

patients all underwent standard-of-care RT for their disease (*i.e.*, the hypoxia-based IMRT plans were generated off-line).

CT simulation

The patients underwent treatment simulation in the treatment position with individualized head, neck, and shoulder Aquaplast immobilization masks (Orfit, Wijnegem, Belgium). A CT scan with 3-mm slices was acquired encompassing the tumor using commercial software (AcQSim, Philips, Andover, MA). An isocenter was determined at simulation, and permanent skin marks were placed to ensure proper repositioning. To further minimize patient misalignment, marks were also drawn on the flat insert to ensure proper repositioning of the immobilization hardware. Finally, small CT markers were placed on the patient's immobilization device to assist in image registration. Patients subsequently underwent PET/CT with the same immobilization devices.

FDG-PET/CT scans

Fluorodeoxyglucose was prepared and injected intravenously (15 mCi) in patients who had been in a fasting state for ≥ 6 h at the Nuclear Medicine Suite. At 45–60 min after injection, PET/CT scanning was performed, on the same day as the CT simulation. Patients were placed in the same treatment position on the GE Discovery LS PET/CT scanner (GE Medical Systems, Waukesha, WI) consisting of an Advance NXi PET and a LightSpeed CT unit. The LightSpeed is a four-slice CT scanner with a 50 cm transaxial field of view (FOV) and slice thicknesses of 0.63–20.0 mm. The tube current can be varied from 10 to 440 mA and the tube voltage from 80 to 140 kV, in 20-kV increments. The PET Advance NXi scanner is a whole-body scanner with a transaxial FOV of 55 cm and an axial FOV of 15.2 cm. The scanner has septa for two-dimensional high-resolution image acquisition. The intrinsic resolution is 4.2 mm full-width half-maximum.

To ensure accurate co-registration of the CT data sets from the CT simulation and PET/CT images, seven fiducial markers were placed for each patient on the immobilization mask: one at the isocenter, three at the chin, and three at the shoulder level. A 3 min/FOV scan was acquired for the FDG-PET portion of the study.

Radiopharmaceutical synthesis of ^{18}F -FMISO

Fluorine-18-labeled fluoride was produced by the Memorial Sloan-Kettering Cancer Center/Cornell Cyclotron Radiochemistry Core Facility by proton irradiation of an enriched ^{18}O water target in a small-volume niobium chamber with an approximate specific activity of 1–2 Ci/ μmol at the end of the bombardment time and tested for quality assurance within the Cyclotron/Radiochemistry Core Facility. For PET imaging to assess tumor uptake and biodistribution, 10.4 ± 1.1 mCi in 1–3 mL of sterile saline was administered intravenously. Blood samples were obtained immediately before and after the PET/CT session. Human use of ^{18}F -FMISO was covered by an investigational drug authorization from the Memorial Sloan-Kettering Cancer Center Radioactive Drug Research Committee.

Measured aliquots of each blood sample were counted in triplicate using a CompuGamma CS Gamma Counter (LKB-Wallac, Turku, Finland), and the net count rates were converted to the activity concentration (Bq/cc) decay corrected to the time of injection. Blood standard uptake values were also calculated.

This portion of the feasibility study involved one injection of 370 MBq of ^{18}F -FMISO before PET/CT scanning. The urinary bladder wall was subject to the largest dose of 0.78 cGy after one imaging session (24). In addition, an additional CT scan that accompanied the ^{18}F -FMISO PET scan contributed an additional 0.5-cGy whole body dose. The dose to the eyes from

one ^{18}F -FMISO PET scan and one CT scan was 0.57 cGy plus 0.5 cGy for a total of 1.07 cGy (24). These radiation doses were insignificant additions to the standard therapeutic dose of 7,000 cGy. The complete biodistribution data on ^{18}F -FMISO was obtained for 60 patients at the University of Washington School of Medicine, and dosimetry was performed. The normal organ doses absorbed after ^{18}F -FMISO administration have been published by Graham *et al.* (24).

^{18}F -FMISO PET/CT scanning

One day after FDG-PET/CT and CT simulation, ^{18}F -FMISO PET/CT was performed. No fasting state was required. ^{18}F -FMISO was injected into the patients approximately 2–2.5 h before scanning. Patients underwent scanning with the same immobilization device as used for CT simulation. Each of the ^{18}F -FMISO studies covered two PET axial FOVs at the tumor position, 8 min/FOV. The mean acquired ^{18}F -FMISO PET/CT data for all patients was at 162 min after injection. The ^{18}F -FMISO emission data were corrected for attenuation, scatter, and random counts and subsequently reconstructed using the same parameters as used for standard FDG reconstruction clinically (28 subsets, two iterations, postfilter, 6.0 mm full-width half-maximum, loop filter, 4.3 mm full-width half-maximum).

Registration of treatment planning CT and PET/CT and determination of GTV_h

The GTV delineation was determined not only from FDG-PET/CT, but also from the clinical examination and other available imaging (*i.e.*, diagnostic CT with contrast or magnetic resonance imaging) findings. The defined GTV was subsequently registered and copied to the CT portion of the ^{18}F -FMISO scan. This was done with the help of fiducial markers and image registration using ImgReg between the ^{18}F -FMISO and FDG-PET/CT scans. Image registration was done using information from the CT image sets by manually aligning the CT portion of the FDG scan with the CT portion of the ^{18}F -FMISO scan. The defined GTVs, as contoured on the CT portion of the FDG and the CT portion of the ^{18}F -FMISO PET scans, were then rigidly co-registered using the mutual information registration technique. The defined GTV also contained the segmented GTV drawn using the iterative segmentation technique of Nehmeh *et al.* (45). Because the blood values were also expressed in microcuries per milliliter, pixel-by-pixel calculation of the T/B activity ratio for all image planes was done. Therefore, the GTV_h , denoting the hypoxic subvolume, was defined as

$$\text{GTV}_h = \frac{{}^{18}\text{F-FMISO_GTV}_{\text{T/B} \geq 1.3}}{\text{FDG_GTV}}$$

All image information was subsequently transferred and aligned with the treatment planning CT scan. An example of the multimodality imaging acquisition, processing, and registration necessary for ^{18}F -FMISO PET/CT-guided IMRT is shown using the ^{18}F -FMISO, FDG, and CT images for 1 HNC patient in Fig. 1. Both FDG and ^{18}F -FMISO uptake was heterogeneous, with similarities or differences between the distributions of the two tracers quantified using correlation measures of the spatial voxel intensities between the respective images.

Treatment planning for ^{18}F -FMISO PET/CT-guided IMRT

In addition to the tumor targets (GTV , GTV_h) and various normal tissues contours, the clinical target volume (CTV) was defined as any microscopic disease at risk of disease involvement. Depending on the clinical scenario, the CTV was divided into high- and low-risk CTVs. A 3–5-mm margin was applied to all of these target volumes, except for the GTV_h , to account for organ motion and patient setup error. Thus, several separate planning target volumes (PTVs) were defined, including PTV_{GTV} and $\text{PTV}_{\text{high-risk CTV}}$. A $\text{PTV}_{\text{low-risk CTV}}$, with the

corresponding low-risk CTV, was delineated when necessary. A total dose of 70 Gy was prescribed to the PTV_{GTV} and 59.4 Gy to the PTV_{high-risk CTV}. When clinically indicated, 54 Gy was prescribed to the PTV_{low-risk CTV}. A dose of 84 Gy (20% greater than the primary GTV dose) was prescribed to the GTV_h. All targets were treated simultaneously for 33 fractions. Treatment plans were generated respecting the normal tissue tolerance (Table 1). We also identified 2 patients in whom additional dose escalation (50% greater than the primary GTV dose) to the GTV_h was done. The prescription for both patients was 105 Gy to the GTV_h, with a simultaneous dose of 70 Gy to the PTV_{GTV} and 59.4 Gy to the PTV_{high-risk CTV}. Table 1 also lists the treatment planning parameters used to perform ¹⁸F-FMISO PET-guided IMRT. These are the constraints routinely used in our clinic to treat HNC.

Results

The heterogeneous distribution of ¹⁸F-FMISO within the GTV demonstrated that the severity of hypoxia varied throughout the GTV. Figure 2 is an example of the delineation of the GTV determined from the clinical examination/imaging findings, including the FDG-PET/CT-defined volume and GTV_h determined from the ¹⁸F-FMISO PET/CT-defined volume. Both these defined volumes were shown in the treatment planning CT used to perform hypoxia-guided IMRT planning. We were able to demonstrate the feasibility of ¹⁸F-FMISO PET/CT-guided IMRT for 10 HNC patients. Figures 3 (supraglottic carcinoma) and 4 (oropharyngeal carcinoma) are examples of ¹⁸F-FMISO PET/CT-guided IMRT plans. Figures 3a-1 and 4a-1 are axial slices of the clinically accepted plans in which the PTV_{GTV} received 70 Gy, the PTV_{high risk} received 59.4 Gy, and the PTV_{low risk} received 54 Gy. In addition to the above prescriptions, 84 Gy was also delivered to the GTV_h (Fig. 3a-2, 3b, and 3c and Fig. 4a-2, 4b, and 4c [axial, sagittal, and coronal slices, respectively]). Note that the beam angles used in the hypoxia dose painting plan were the exact angles used in the clinically accepted plan. The only difference was in the constraints applied to achieve the desired dose distributions. Very few differences were present between the plans, except that the PTVs of the hypoxia plan in terms of the dose to the maximal point, minimal dose to hottest 5% of the volume, and mean dose received a greater total dose than in the clinically accepted plan. Thus, the hypoxia plan was "hotter." Figure 4d shows a dose-volume histogram (DVH) of the hypoxia-guided IMRT plan.

Table 2 summarizes the average of all the DVHs for all 10 patients in this study, in which each DVH value is the average of all 10 patients' DVH for the particular structure. No attempts were made to further refine the clinically accepted plan. The planner used a tighter constraint during hypoxia dose painting. On average, there were essentially very few differences between the two plans in terms of normal tissues doses, with the dose to the maximal point, minimal dose to hottest 5% of the volume, and mean dose greater in the hypoxia plans than in the clinical plans. Although these doses were greater, they were encompassed within the GTV and, largely, were encompassed within the GTV_h.

After demonstrating the feasibility of using ¹⁸F-FMISO PET-guided IMRT in which the GTV_h received 84 Gy, we increased the GTV_h dose to 105 Gy (50% increase in the dose delivered to the primary tumor) (30) for 2 patients. The GTV_h received 318 cGy/fraction. One patient had a relatively small tumor volume, along with a small GTV_h, and the other had a larger tumor volume with a correspondingly larger GTV_h. We had no difficulty in delivering 105 Gy to the GTV_h in the patient with the smaller tumor volume (Fig. 5). We were, however, unable to meet the normal tissue constraints for the larger tumor volume when trying to escalate the GTV_h dose to 105 Gy. In this patient who had a large oropharyngeal tumor, the best achievable escalated dose to the GTV_h was 100 Gy, 43% greater than the primary tumor dose, without compromising normal tissue tolerance (Fig. 6).

Discussion

Improving LRC, overall survival, and patient quality of life have always been the goals of HNC treatment (46–54). However, some patients still die of their disease, particularly those with larger tumors. The preliminary tumor control in patients treated with IMRT has been promising; however, when analyzing the patterns of failure, studies have shown that tumors tend to recur within the GTV, which can lead to greater distant metastasis rates (35,36,55–59).

Investigators have suggested increasing the dose delivered to the GTV to further improve LRC (35,36,60). However, owing to fear of unwarranted complications that could result from an increased radiation dose to the GTV, such a strategy has not been implemented in clinical trials. A more rationale approach might be to selectively increase the dose only to subregions of the tumor known to exhibit greater radioresistance (*i.e.*, hypoxic subvolumes) (4,8,10,21,42). In particular, many investigators have shown that the presence of hypoxia compromised tumor control, disease-free survival, and overall survival (2,9,15,61).

Rasey *et al.* (25) reported on the first ^{18}F -FMISO PET-image-based hypoxia measurement. Misonidazole is preferentially and metabolically reduced and entrapped within hypoxic, but not aerobic, cells. Pimonidazole is a well-established hypoxia marker for immunohistochemical investigations (62). Because the functional binding mechanisms of pimonidazole and ^{18}F -FMISO are similar, the distribution of ^{18}F -FMISO is expected to colocalize with pimonidazole (62). This has been confirmed through studies performed in our laboratory in which frozen tissue sections from R3327-AT Dunning rat prostate tumor-bearing animals, co-injected with pimonidazole and ^{18}F -FMISO, showed a high correlation between the fluorescence intensity of the anti-pimonidazole antibody with the digital autoradiographic intensity of the ^{18}F hypoxia tracer. Other investigators have identified different hypoxia tracers such as ^{64}Cu -ATSM (63–66). Groups using each of these hypoxia radiotracers have discussed their potential for RT dose painting as proposed by Ling *et al.* (40). Our clinical study focused on the use of ^{18}F -FMISO because our *in vitro* (67) and *in vivo* (17) analyses of ^{64}Cu -ATSM and ^{18}F -FMISO demonstrated unresolved tumor cell line uptake kinetic dependence for the ^{64}Cu -ATSM tracer.

In the present study, ^{18}F -FMISO PET images were used, subject to a 1.3 T/B threshold to define the GTV_h . The goal of this study was to investigate the feasibility of dose painting to these GTV_h regions. We demonstrated the ability to achieve a boost dose of 20% in excess of the primary tumor dose in 10 HNC patients without compromising the normal tissue tolerance. Attempts to plan a GTV_h dose of 50% greater than the primary tumor dose was successful in 1 of 2 patients for whom it was attempted, with acceptable normal tissue dose constraints. The patient with the larger GTV in our example contained larger volumes of GTV_h , rendering it difficult to achieve a tumoricidal dose of 105 Gy without exceeding the normal tissue tolerance. IMRT merely manipulates the isodose curves; therefore, the greater the dose delivered to a larger volume, the more difficult to minimize the dose delivered to the surrounding normal tissue without exceeding its tolerance. In theory, in patients for whom the GTV is large but the GTV_h is small, it might still be feasible to deliver a tumoricidal dose of 105 Gy. Perhaps based on the geometry, volume, and location of the different head-and-neck tumors, a differential increase in the dose delivered to the GTV_h should also be considered and should be patient specific. Additional studies examining the clinical, radiographic, and biologic behavior of each tumor in determining the necessary doses needed to overcome hypoxia resistance are warranted.

Tirapazamine has shown great promise in targeting hypoxia. A Phase I trial of concurrent tirapazamine and RT in treating advanced HNC was performed at the Peter MacCallum Cancer Institute. All patients underwent ^{18}F -FMISO PET, obtained 2 h after radiotracer administration,

to provide evidence of tumor hypoxia. Of the 15 patients studied, 14 had detectable hypoxia at baseline. Of the 14 patients with an initially positive ^{18}F -MISO PET scan, 13 showed complete resolution of the abnormality within 4–5 weeks of treatment (68,69). The rapid normalization of ^{18}F -FMISO PET findings suggests successful treatment of the hypoxic component. A subsequent Phase II trial was performed that showed that patients with hypoxia detected by ^{18}F -FMISO PET imaging treated with tirapazamine-containing chemoradiotherapy was associated with greater LRC compared with those patients receiving a non-tirapazamine-containing chemoradiotherapy regimen (70). However, systemic toxicity, muscle cramping, nausea, and fatigue have precluded its routine use in HNC patients. Consequently, subsequent tirapazamine-based clinical trials, aimed at targeting hypoxia, have been closed because of the unexpected toxicities and deaths. Therefore, hypoxia dose painting IMRT might be a more attractive option, with potentially less toxicity, than treating these patients with multiple co-morbidities induced by systemic agents such as tirapazamine.

Although hypoxia dose painting is one method used to overcome hypoxia, one must not overlook the potential risks associated with this treatment approach. The increased dose might result in an increased risk of a second cancer where the greater integral dose is delivered to the patient. This issue has been questioned by investigators since the advent of IMRT because of concern for this theoretical risk (71). No greater rates of second malignancies have been reported; however, one must keep this important issue in mind when implementing hypoxia dose painting. In addition, potential hot spots (areas receiving a higher radiation dose) can occur in the nonconstrained normal tissue with dose escalation. To prevent these unwarranted hot spots from occurring, every effort must be made to constrain all surrounding normal tissue before plan acceptance. Therefore, before the routine implementation of hypoxia dose painting in the clinic, one must examine these issues. One must weigh the benefits of hypoxia dose painting against these risks.

The present feasibility study was based on several assumptions. First, the treatment plans were done using on a single ^{18}F -FMISO PET scan performed at ~ 2.5 h after injection. Studies by others (72,73) have shown potential limitations with single time point imaging and have proposed a dynamic scanning approach. In the latter method, the kinetic information of the tracer uptake and retention behavior in each PET image voxel is used to generate parametric maps of putative hypoxia tracer trapping using compartmental models of the tracer binding chemistry (71,72). Second, we assumed that the single ^{18}F -FMISO image reflected a static distribution of hypoxia within the tumor and did not consider contributions from acute hypoxia. The results presented in this report assumed ^{18}F -FMISO targeting of chronic hypoxia only. However, variations in the distribution of hypoxia uptake, between the time of PET/CT simulation and the start of treatment, whether from acute hypoxia or changes in chronic hypoxia, need to be determined. Such a study is underway at our center to determine the constancy of the hypoxic sub-volume by repeat ^{18}F -MISO PET images before initiation of the first RT fraction. This is an essential prerequisite before the clinical implementation of hypoxia dose painting IMRT. Third, the small potential GTV_h within the GTV will place even greater accuracy constraints on tumor localization, necessitating image guidance during RT. This is the largest study of the feasibility of hypoxia-guided dose painting IMRT in a cohort of HNC patients, it is the first step in a careful process aimed toward the clinical implementation of radiobiologically based IMRT planning.

Conclusion

Hypoxia, detected by ^{18}F -FMISO PET scanning, has been shown to decrease LRC of HNC. In our study, we have demonstrated the feasibility of dose escalating to the GTV_h within the GTV without compromising normal tissue sparing using ^{18}F -FMISO PET/CT-guided dose painting IMRT in a cohort of HNC patients. This information has provided important data for

subsequent hypoxia-guided IMRT trials, with the ultimate goal of further improving LRC in HNC. Additional studies to ensure the invariance of the ^{18}F -FMISO PET hypoxia uptake, accurate tumor target localization, and tumor reoxygenation kinetics are necessary before the routine implementation of ^{18}F -FMISO hypoxia dose painting in the RT clinic.

Acknowledgments

Supported by the American Society for Therapeutic Radiology and Oncology (ASTRO) Junior Investigator Award.

References

1. Terris DJ. Head and neck cancer: The importance of oxygen. *Laryngoscope* 2000;110:697–707. [PubMed: 10807350]
2. Brizel DM, Sibley GS, Prosnitz LR, et al. Tumor hypoxia adversely affects the prognosis of carcinoma of the head and neck. *Int J Radiat Oncol Biol Phys* 1997;38:285–289. [PubMed: 9226314]
3. Hockel M, Vorndran B, Schlenger K, et al. Tumor oxygenation: A new predictive parameter in locally advanced cancer of the uterine cervix. *Gynecol Oncol* 1993;51:141–149. [PubMed: 8276286]
4. Isa AY, Ward TH, West CM, et al. Hypoxia in head and neck cancer. *Br J Radiol* 2006;79:791–798. [PubMed: 16854964]
5. Kaanders JH, Wijffels KI, Marres HA, et al. Pimonidazole binding and tumor vascularity predict for treatment outcome in head and neck cancer. *Cancer Res* 2002;62:7066–7074. [PubMed: 12460928]
6. Becker A, Hansgen G, Bloching M, et al. Oxygenation of squamous cell carcinoma of the head and neck: Comparison of primary tumors, neck node metastases, and normal tissue. *Int J Radiat Oncol Biol Phys* 1998;42:35–41. [PubMed: 9747817]
7. Gray LH, Conger AD, Ebert M. The concentration of oxygen dissolved in tissues at the time of irradiation as a factor in radiotherapy. *Br J Radiol* 1953;26:638–648. [PubMed: 13106296]
8. Graeber TG, Osmanian C, Jacks T, et al. Hypoxia-mediated selection of cells with diminished apoptotic potential in solid tumours. *Nature* 1996;379:88–91. [PubMed: 8538748]
9. Nordmark M, Bentzen SM, Rudat V, et al. Prognostic value of tumor oxygenation in 397 head and neck tumors after primary radiation therapy: An international multi-center study. *Radiother Oncol* 2005;77:18–24. [PubMed: 16098619]
10. Nordmark M, Overgaard J. A confirmatory prognostic study on oxygenation status and loco-regional control in advanced head and neck squamous cell carcinoma treated by radiation therapy. *Radiother Oncol* 2000;57:39–43. [PubMed: 11033187]
11. Brizel DM, Dodge RK, Clough RW, et al. Oxygenation of head and neck cancer: Changes during radiotherapy and impact on treatment outcome. *Radiother Oncol* 1999;53:113–117. [PubMed: 10665787]
12. Hockel M, Knoop C, Schlenger K, et al. Intratumoral pO_2 predicts survival in advanced cancer of the uterine cervix. *Radiother Oncol* 1993;26:45–50. [PubMed: 8438086]
13. Tatum JL, Kelloff GJ, Gillies RJ. Hypoxia: Importance in tumor biology, noninvasive measurement by imaging, and value of its measurement in the management of cancer therapy. *Int J Radiat Biol* 2006;82:699–757. [PubMed: 17118889]
14. Chapman JD, Zanzonico P, Ling CC. On measuring hypoxia in individual tumors with radiolabeled agents. *J Nucl Med* 2001;42:1653–1655. [PubMed: 11696634]
15. Nordmark M. Direct measurements of tumor-tissue pO_2 : A way of selecting patients for hyperoxic treatment. *Strahlenther Onkol* 1996;172(Suppl. 2):8–9. [PubMed: 8946036]
16. Gagel B, Reinartz P, Dimartino E, et al. pO_2 Polarography versus positron emission tomography (^{18}F fluoromisonidazole, ^{18}F -2-fluoro-2'-deoxyglucose): An appraisal of radiotherapeutically relevant hypoxia. *Strahlenther Onkol* 2004;180:616–622. [PubMed: 15480509]
17. O'Donoghue JA, Zanzonico P, Pugachev A, et al. Assessment of regional tumor hypoxia using ^{18}F -fluoromisonidazole and ^{64}Cu (II)-diacetyl-bis(N4-methylthiosemicarbazone) positron emission tomography: Comparative study featuring microPET imaging, pO_2 probe measurement, autoradiography, and fluorescent microscopy in the R3327-AT and FaDu rat tumor models. *Int J Radiat Oncol Biol Phys* 2005;61:1493–1502. [PubMed: 15817355]

18. Le QT, Kovacs MS, Dorie MJ, et al. Comparison of the comet assay and the oxygen microelectrode for measuring tumor oxygenation in head-and-neck cancer patients. *Int J Radiat Oncol Biol Phys* 2003;56:375–383. [PubMed: 12738312]
19. Brown JM, Siim BG. Hypoxia-specific cytotoxins in cancer therapy. *Semin Radiat Oncol* 1996;6:22–36. [PubMed: 10717159]
20. Bussink J, Kaanders JH, van der Kogel AJ. Tumor hypoxia at the micro-regional level: Clinical relevance and predictive value of exogenous and endogenous hypoxic cell markers. *Radiother Oncol* 2003;67:3–15. [PubMed: 12758235]
21. Chao KS, Bosch WR, Mutic S, et al. A novel approach to overcome hypoxic tumor resistance: Cu-ATSM-guided intensitymodulated radiation therapy. *Int J Radiat Oncol Biol Phys* 2001;49:1171–1182. [PubMed: 11240261]
22. Koch CJ, Evans SM. Non-invasive PET and SPECT imaging of tissue hypoxia using isotopically labeled 2-nitroimidazoles. *Adv Exp Med Biol* 2003;510:285–292. [PubMed: 12580442]
23. Rajendran JG, Schwartz DL, O'Sullivan J, et al. Tumor hypoxia imaging with [F-18] fluoromisonidazole positron emission tomography in head and neck cancer. *Clin Cancer Res* 2006;12:5435–5441. [PubMed: 17000677]
24. Graham MM, Peterson LM, Link JM, et al. Fluorine-18-fluoro-misonidazole radiation dosimetry in imaging studies. *J Nucl Med* 1997;38:1631–1636. [PubMed: 9379204]
25. Rasey JS, Koh WJ, Grierson JR, et al. Radiolabelled fluoromisonidazole as an imaging agent for tumor hypoxia. *Int J Radiat Oncol Biol Phys* 1989;17:985–991. [PubMed: 2808061]
26. Wen B, Burgman P, Zanzonico P, et al. A preclinical model for noninvasive imaging of hypoxia-induced gene expression: Comparison with an exogenous marker of tumor hypoxia. *Eur J Nucl Med Mol Imaging* 2004;31:1530–1538. [PubMed: 15378285]
27. Koh WJ, Rasey JS, Evans ML, et al. Imaging of hypoxia in human tumors with [F-18] fluoromisonidazole. *Int J Radiat Oncol Biol Phys* 1992;22:199–212. [PubMed: 1727119]
28. Adams GE, Stratford IJ. Hypoxia-mediated nitro-heterocyclic drugs in the radio- and chemotherapy of cancer: An overview. *Biochem Pharmacol* 1986;35:71–76. [PubMed: 2934067]
29. Rasey JS, Koh WJ, Evans ML, et al. Quantifying regional hypoxia in human tumors with positron emission tomography of [18F]fluoromisonidazole: A pretherapy study of 37 patients. *Int J Radiat Oncol Biol Phys* 1996;36:417–428. [PubMed: 8892467]
30. Popple RA, Ove R, Shen S. Tumor control probability for selective boosting of hypoxic subvolumes, including the effect of reoxygenation. *Int J Radiat Oncol Biol Phys* 2002;54:921–927. [PubMed: 12377346]
31. Chao KS, Deasy JO, Markman J, et al. A prospective study of salivary function sparing in patients with head-and-neck cancers receiving intensity-modulated or three-dimensional radiation therapy: Initial results. *Int J Radiat Oncol Biol Phys* 2001;49:907–916. [PubMed: 11240231]
32. Lee N, Xia P, Quivey JM, et al. Intensity-modulated radiotherapy in the treatment of nasopharyngeal carcinoma: An update of the UCSF experience. *Int J Radiat Oncol Biol Phys* 2002;53:12–22. [PubMed: 12007936]
33. Eisbruch A, Dawson LA, Kim HM, et al. Conformal and intensity modulated irradiation of head and neck cancer: The potential for improved target irradiation, salivary gland function, and quality of life. *Acta Otorhinolaryngol Belg* 1999;53:271–275. [PubMed: 10635407]
34. Dawson LA, Anzai Y, Marsh L, et al. Patterns of local-regional recurrence following parotid-sparing conformal and segmental intensity-modulated radiotherapy for head and neck cancer. *Int J Radiat Oncol Biol Phys* 2000;46:1117–1126. [PubMed: 10725621]
35. Lee N, Xia P, Fischbein NJ, et al. Intensity-modulated radiation therapy for head-and-neck cancer: The UCSF experience focusing on target volume delineation. *Int J Radiat Oncol Biol Phys* 2003;57:49–60. [PubMed: 12909215]
36. Chao KS, Ozyigit G, Tran BN, et al. Patterns of failure in patients receiving definitive and postoperative IMRT for head-and-neck cancer. *Int J Radiat Oncol Biol Phys* 2003;55:312–321. [PubMed: 12527043]
37. Alber M, Paulsen F, Eschmann SM, et al. On biologically conformal boost dose optimization. *Phys Med Biol* 2003;48:N31–N35. [PubMed: 12587912]

38. Grosu AL, Piert M, Weber WA, et al. Positron emission tomography for radiation treatment planning. *Strahlenther Onkol* 2005;181:483–499. [PubMed: 16044216]
39. Zanzonico P. PET-based biological imaging for radiation therapy treatment planning. *Crit Rev Eukaryot Gene Expr* 2006;16:61–101. [PubMed: 16584383]
40. Ling CC, Humm J, Larson S, et al. Towards multidimensional radiotherapy (MD-CRT): Biological imaging and biological conformality. *Int J Radiat Oncol Biol Phys* 2000;47:551–560. [PubMed: 10837935]
41. Malinen E, Sovik A, Hristov D, et al. Adapting radiotherapy to hypoxic tumours. *Phys Med Biol* 2006;51:4903–4921. [PubMed: 16985278]
42. Rajendran JG, Hendrickson KRG, Muzi M, et al. Hypoxia imaging-directed radiation treatment planning. *Eur J Nucl Med Mol Imaging* 2006;33:S44–S53.
43. Rajendran JG, Mankoff DA, O'Sullivan F, et al. Hypoxia and glucose metabolism in malignant tumors: Evaluation by [18F]fluoromisonidazole and [18F]fluorodeoxyglucose positron emission tomography imaging. *Clin Cancer Res* 2004;10:2245–2252. [PubMed: 15073099]
44. Rajendran JG, Wilson DC, Conrad EU, et al. [(18)F]FMISO and [(18)F]FDG PET imaging in soft tissue sarcomas: Correlation of hypoxia, metabolism and VEGF expression. *Eur J Nucl Med Mol Imaging* 2003;30:695–704. [PubMed: 12632200]
45. Nehmeh S, Hossam EZ, Yusuf E, et al. An iterative technique for lesion segmentation in PET images. *J Nucl Med* 2006;47:364P.
46. Parsons JT, Mendenhall WM, Stringer SP, et al. Squamous cell carcinoma of the oropharynx: Surgery, radiation therapy, or both. *Cancer* 2002;94:2967–2980. [PubMed: 12115386]
47. Soo KC, Tan EH, Wee J, et al. Surgery and adjuvant radiotherapy vs concurrent chemoradiotherapy in stage III/IV nonmetastatic squamous cell head and neck cancer: A randomised comparison. *Br J Cancer* 2005;93:279–286. [PubMed: 16012523]
48. Fu KK. Combined radiotherapy and chemotherapy for nasopharyngeal carcinoma. *Semin Radiat Oncol* 1998;8:247–253. [PubMed: 9873102]
49. Goldsmith DB, West TM, Morton R. HLA associations with nasopharyngeal carcinoma in Southern Chinese: A meta-analysis. *Clin Otolaryngol Allied Sci* 2002;27:61–67. [PubMed: 11903375]
50. Huncharek M, Kupelnick B. Combined chemoradiation versus radiation therapy alone in locally advanced nasopharyngeal carcinoma: Results of a meta-analysis of 1,528 patients from six randomized trials. *Am J Clin Oncol* 2002;25:219–223. [PubMed: 12040275]
51. Kohno N, Kitahara S. Role of chemotherapy in head and neck cancer. *Gan To Kagaku Ryoho* 2001;28:448–453. [PubMed: 11329777]
52. Langendijk JA, Leemans CR, Buter J, et al. The additional value of chemotherapy to radiotherapy in locally advanced nasopharyngeal carcinoma: A meta-analysis of the published literature. *J Clin Oncol* 2004;22:4604–4612. [PubMed: 15542811]
53. Ma BB, Chan AT. Recent perspectives in the role of chemotherapy in the management of advanced nasopharyngeal carcinoma. *Cancer* 2005;103:22–31. [PubMed: 15565580]
54. Pignon JP, Bourhis J, Domenge C, et al. MACH-NC (Meta-Analysis of Chemotherapy on Head and Neck Cancer) Collaborative Group. Chemotherapy added to locoregional treatment for head and neck squamous-cell carcinoma: Three meta-analyses of updated individual data. *Lancet* 2000;355:949–955. [PubMed: 10768432]
55. Nutting C, Dearnaley DP, Webb S. Intensity modulated radiation therapy: A clinical review. *Br J Radiol* 2000;73:459–469. [PubMed: 10884741]
56. Leibel SA, Fuks Z, Zelefsky MJ, et al. Intensity-modulated radiotherapy. *Cancer J* 2002;8:164–176. [PubMed: 12004802]
57. Lin A, Kim HM, Terrell JE, et al. Quality of life after parotid-sparing IMRT for head-and-neck cancer: A prospective longitudinal study. *Int J Radiat Oncol Biol Phys* 2003;57:61–70. [PubMed: 12909216]
58. Chao KS, Majhail N, Huang CJ, et al. Intensity-modulated radiation therapy reduces late salivary toxicity without compromising tumor control in patients with oropharyngeal carcinoma: A comparison with conventional techniques. *Radiother Oncol* 2001;61:275–280. [PubMed: 11730997]
59. Brizel DM, Scully SP, Harrelson JM, et al. Tumor oxygenation predicts for the likelihood of distant metastases in human soft tissue sarcoma. *Cancer Res* 1996;56:941–943. [PubMed: 8640781]

60. Corry J, Rischin D. Strategies to overcome accelerated repopulation and hypoxia—What have we learned from clinical trials? *Semin Oncol* 2004;31:802–808. [PubMed: 15599858]
61. Nordmark M, Overgaard J. Tumor hypoxia is independent of hemoglobin and prognostic for loco-regional tumor control after primary radiotherapy in advanced head and neck cancer. *Acta Oncol* 2004;43:396–403. [PubMed: 15303502]
62. Janssen HL, Hoebbers FJ, Sprong D. Differentiation-associated staining with anti-pimonidazole antibodies in head and neck tumors. *Radiother Oncol* 2004;70:91–97. [PubMed: 15036858]
63. Krause BJ, Beck R, Souvatzoglou M, et al. PET and PET/CT studies of tumor tissue oxygenation. *Q J Nucl Med Mol Imaging* 2006;50:28–43. [PubMed: 16557202]
64. Fujibayashi Y, Cutler CS, Anderson CJ, et al. Comparative studies of Cu-64-ATSM and C-11-acetate in an acute myocardial infarction model: Ex vivo imaging of hypoxia in rats. *Nucl Med Biol* 1999;26:117–121. [PubMed: 10096511]
65. Fujibayashi Y, Taniuchi H, Yonekura Y, et al. Copper-62-ATSM: A new hypoxia imaging agent with high membrane permeability and low redox potential. *J Nucl Med* 1997;38:1155–1160. [PubMed: 9225812]
66. Apisarnthanarax S, Chao KS. Current imaging paradigms in radiation oncology. *Radiat Res* 2005;163:1–25. [PubMed: 15606303]
67. Burgman P, O'Donoghue JA, Lewis JS, et al. Cell line-dependent differences in uptake and retention of the hypoxia-selective nuclear imaging agent Cu-ATSM. *Nucl Med Biol* 2005;32:623–630. [PubMed: 16026709]
68. Rischin D, Peters L, Hicks R, et al. Phase I trial of concurrent tirapazamine, cisplatin, and radiotherapy in patients with advanced head and neck cancer. *J Clin Oncol* 2001;19:535–542. [PubMed: 11208848]
69. Hicks RJ, Rischin D, Fisher R, et al. Utility of FMISO PET in advanced head and neck cancer treated with chemoradiation incorporating a hypoxia-targeting chemotherapy agent. *Eur J Nucl Med Mol Imaging* 2005;32:1384–1391. [PubMed: 16133382]
70. Rischin D, Hicks RJ, Fisher R, et al. Prognostic significance of [18F]-misonidazole positron emission tomography-detected tumor hypoxia in patients with advanced head and neck cancer randomly assigned to chemoradiation with or without tirapazamine: A substudy of Trans-Tasman Radiation Oncology Group Study 98.02. *J Clin Oncol* 2006;24:2098–2104. [PubMed: 16648512]
71. Hall EJ, Wu CS. Radiation-induced second cancers: the impact of 3d-CRT and IMRT. *Int J Radiat Oncol Biol Phys* 2003;56:83–88. [PubMed: 12694826]
72. Thorwarth D, Eschmann SM, Paulsen F, et al. A kinetic model for dynamic [18F]-FMISO PET data to analyse tumour hypoxia. *Phys Med Biol* 2005;50:2209–2224. [PubMed: 15876662]
73. Thorwarth D, Eschmann SM, Scheiderbauer J, et al. Kinetic analysis of dynamic 18F-fluoromisonidazole PET correlates with radiation treatment outcome in head-and-neck cancer. *BMC Cancer* 2005;5:152–161. [PubMed: 16321146]

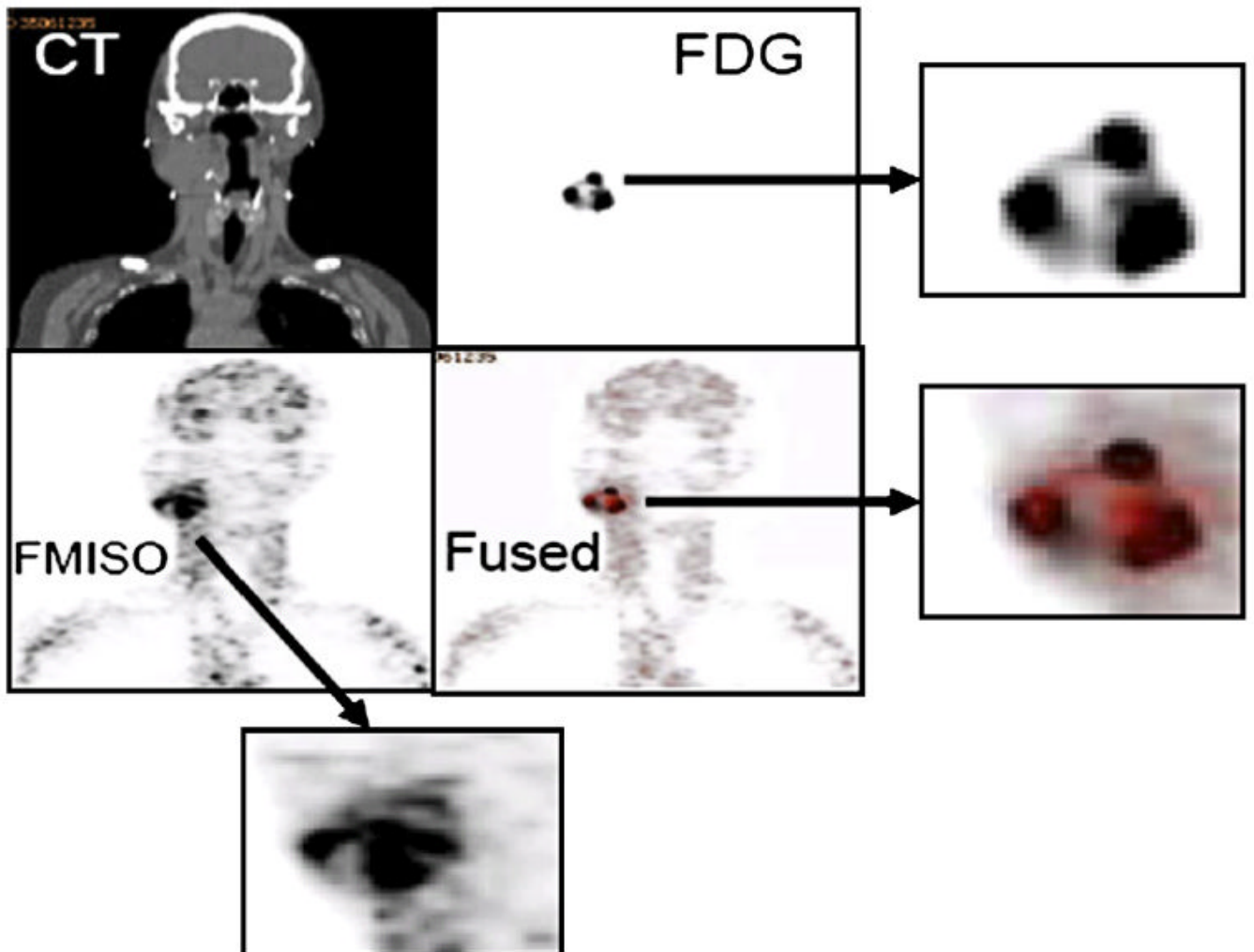


Fig. 1. Example of multimodality image registration of (Top Left) computed tomography (CT), (Top Right) fluorodeoxyglucose (FDG), (Bottom Left) fluorine-18-labeled fluoromisonidazole (^{18}F -FMISO), and (Bottom Right) fused FDG- ^{18}F -FMISO. Three enlarged images (indicated by arrows) of FDG, ^{18}F -FMISO, and fused FDG- ^{18}F -FMISO also shown.

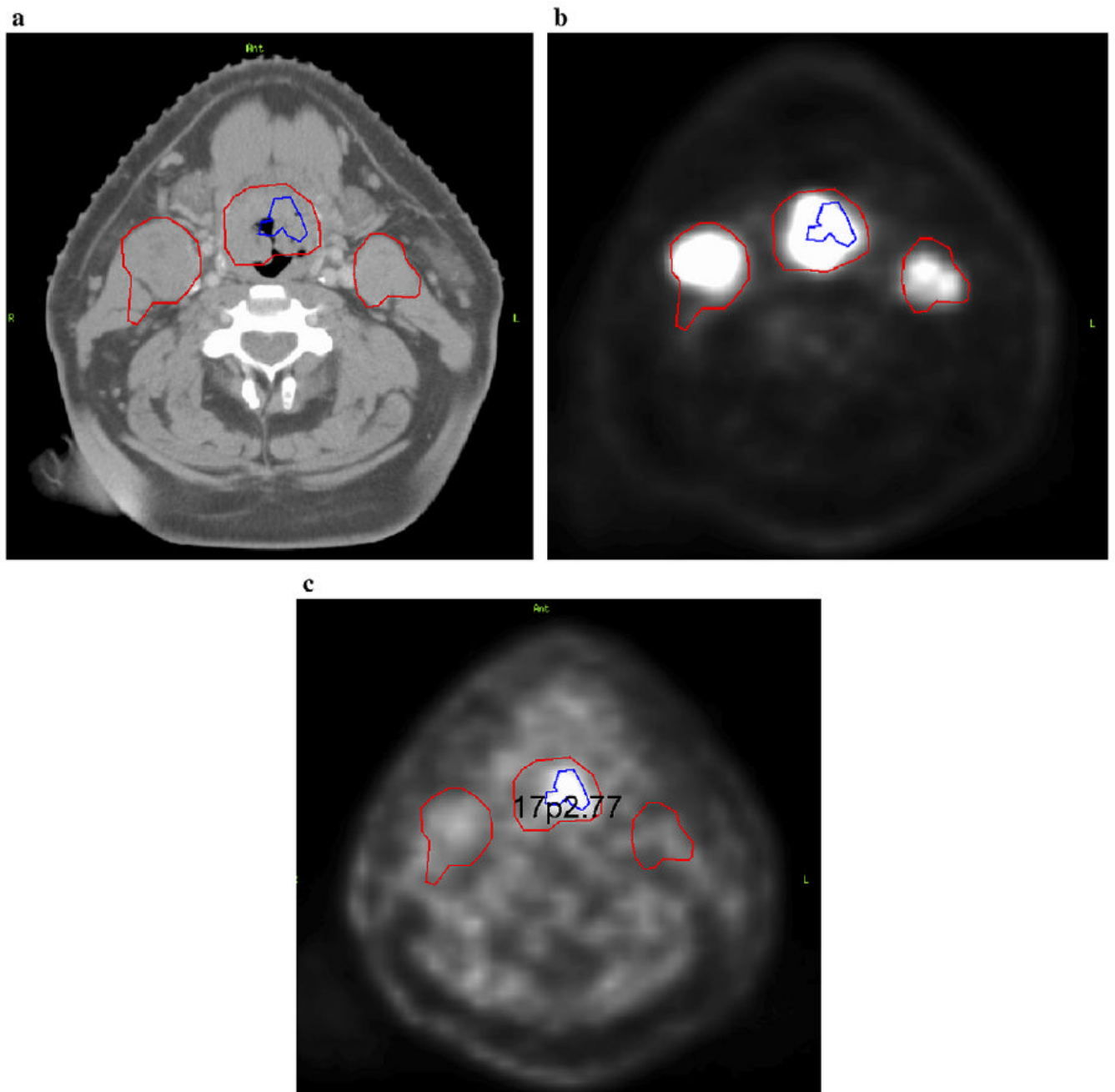


Fig. 2. Example of delineation of gross tumor volume (GTV) and corresponding hypoxic GTV (GTV_h) by fluorodeoxyglucose (FDG) positron emission tomography/computed tomography (PET/CT) and fluorine-18-labeled fluoromisonidazole (^{18}F -FMISO) PET/CT image fusion. (a) CT axial slice, (b) FDG-PET axial scan, and (c) ^{18}F -FMISO PET axial slice.

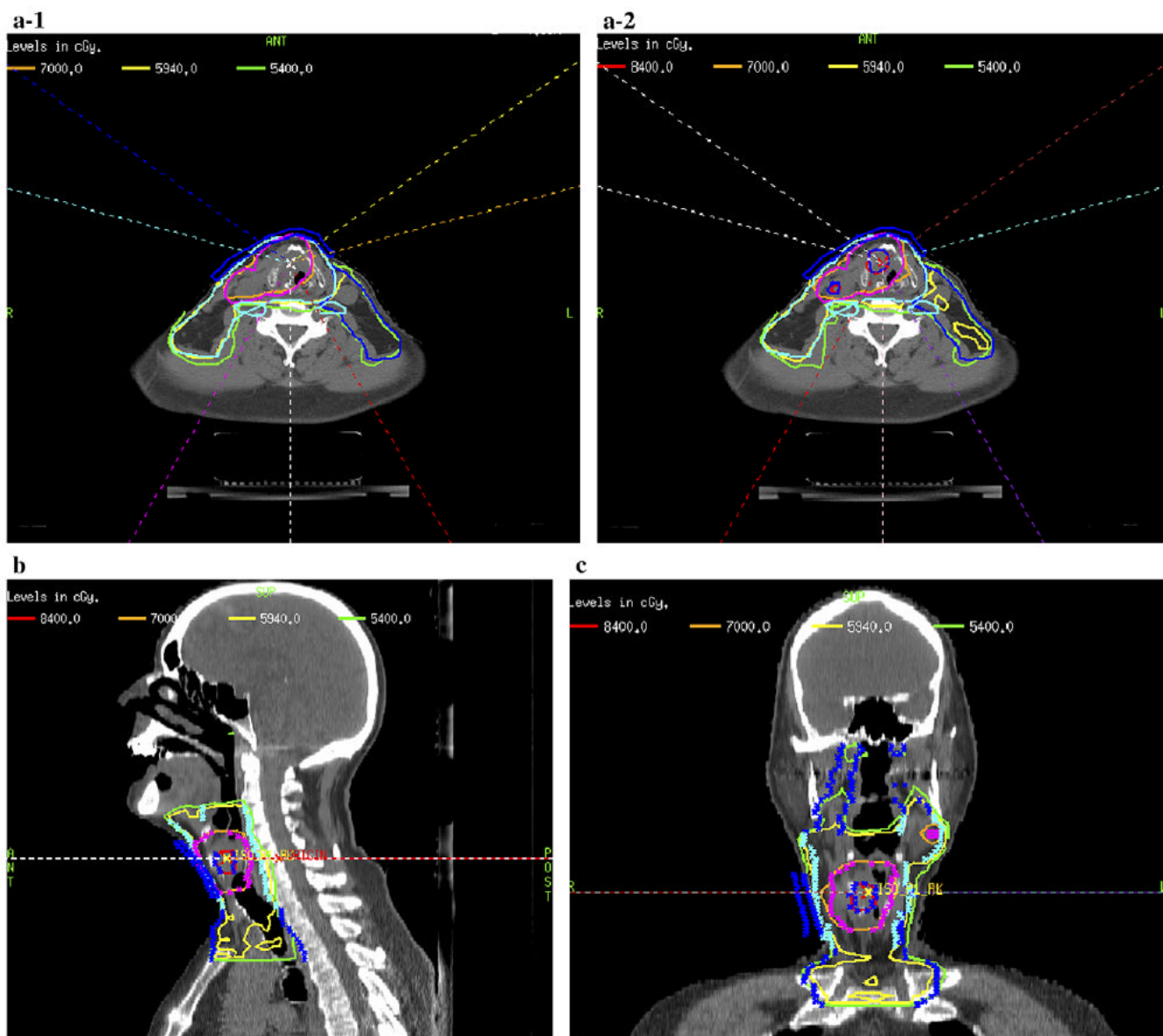


Fig. 3. Example of fluorine-18-labeled fluoromisonidazole (^{18}F -FMISO) positron emission tomography (PET)-guided intensity-modulated radiotherapy (IMRT) plan for locoregionally advanced supraglottic carcinoma. (a) Axial comparison of original clinical plan (a-1) and ^{18}F -FMISO PET-guided IMRT plan (a-2). (b) Sagittal view of ^{18}F -FMISO PET-guided IMRT plan. (c) Coronal view of ^{18}F -FMISO PET-guided IMRT plan.

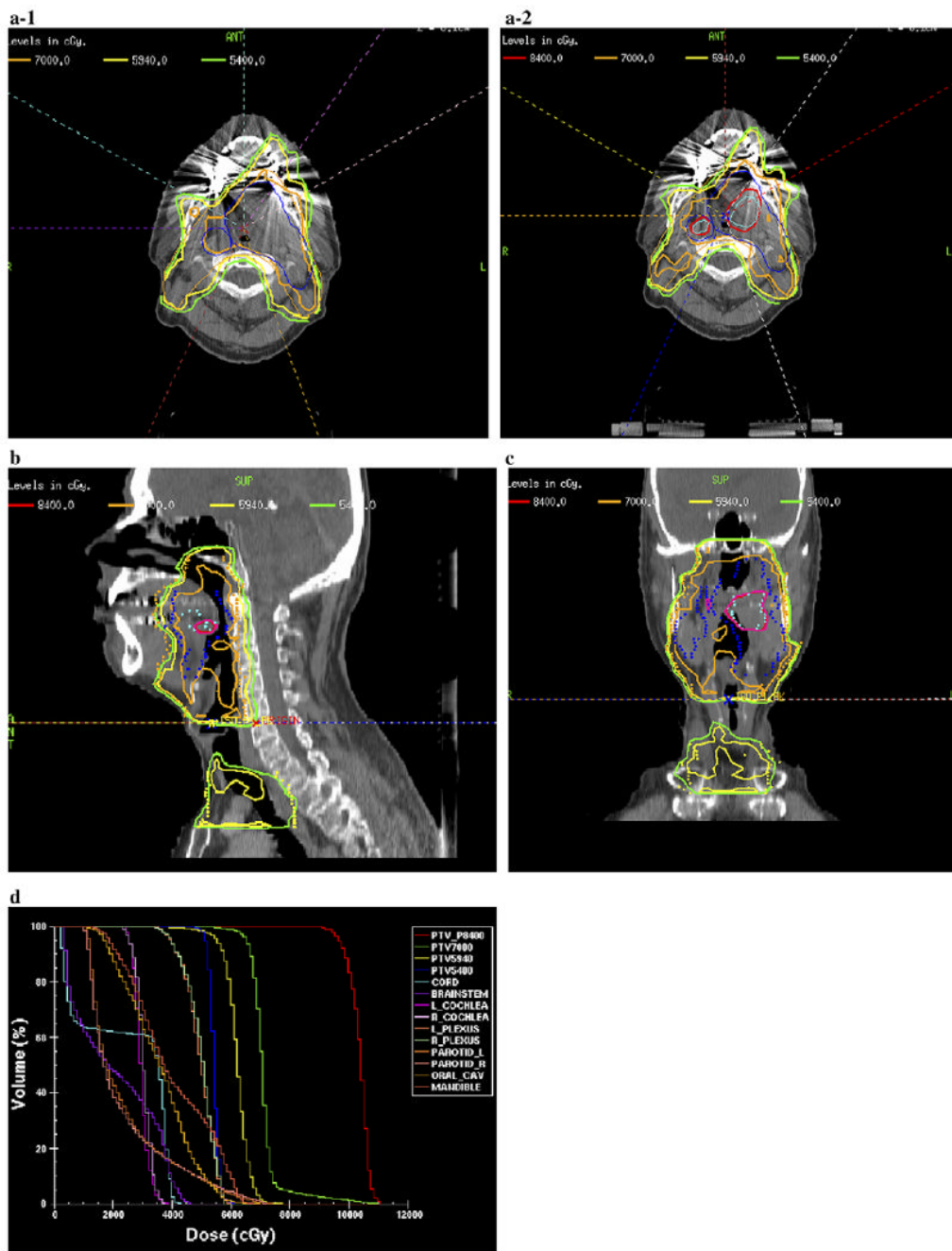


Fig. 4. Second example of fluorine-18–labeled fluoromisonidazole (^{18}F -FMISO) positron emission tomography (PET)–guided intensity-modulated radiotherapy (IMRT) plan for locoregionally advanced oropharyngeal carcinoma. (a) Axial comparison of original clinical plan (a-1) and ^{18}F -FMISO PET–guided IMRT plan (a-2). (b) Sagittal view of ^{18}F -FMISO PET–guided IMRT plan. (c) Coronal view of ^{18}F -FMISO PET–guided IMRT plan. (d) Dose–volume histogram of ^{18}F -FMISO PET–guided IMRT plan.

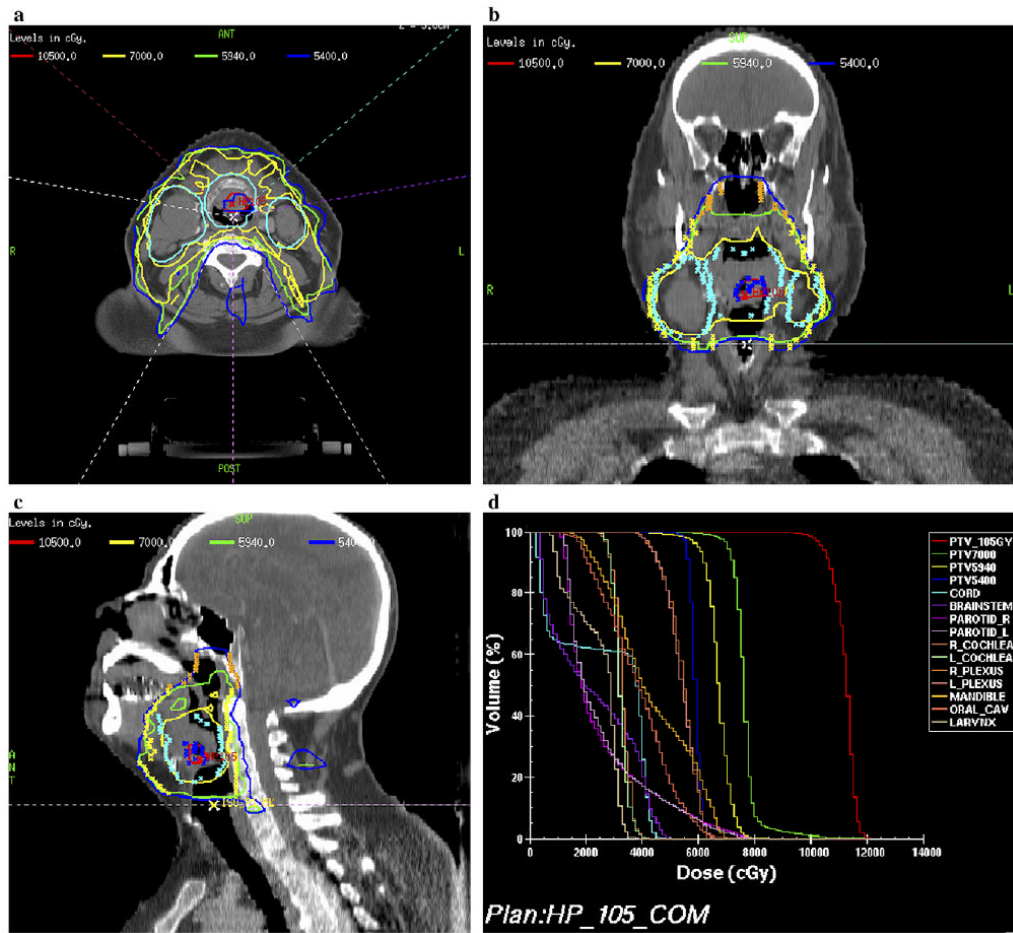


Fig. 5. Example of case in which hypoxic gross tumor volume (GTV_h) escalated to 105 Gy within 33 fractions. (a) Axial, (b) coronal, (c) sagittal views, and (d) dose-volume histogram.

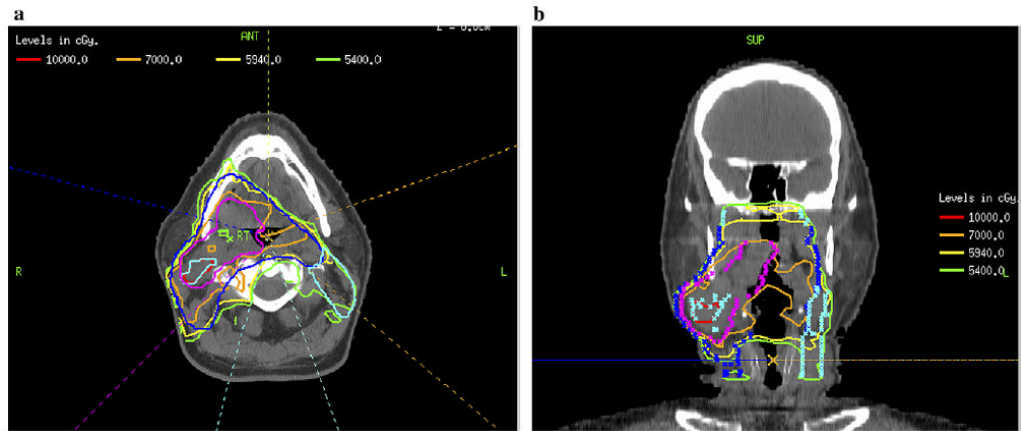


Fig. 6. Example of case in which hypoxic gross tumor volume (GTV_h) escalated to 100 Gy, while preserving normal tissue constraints. (a) Axial. (b) Coronal views.

Table 1

Dose specifications and normal tissue constraints for head and neck cancer

Dose specification	Acceptance criteria
Target coverage	
GTV _h = 84 Gy	D ₉₅ ≥ prescription dose
	D ₀₅ ≤ 108% of prescription dose
PTV _{GTV} = 70 Gy	D ₉₅ ≥ prescription dose
	D ₀₅ ≤ PTV _{GTVh} prescription dose
PTV _{high-risk CTV} = 59.4 Gy	D ₉₅ ≥ prescription dose
	D ₀₅ ≤ PTV _{GTV} prescription dose
PTV _{low-risk CTV} = 54 Gy	D ₉₅ ≥ prescription dose
	D ₀₅ ≤ PTV _{high-risk CTV} prescription dose
Normal tissue constraint	
Spinal cord	Dmax 45 Gy (50 Gy)
Brain stem	Dmax 50 Gy (60 Gy)
Cochlea	Dmax 50 Gy (D ₀₅ ≤ 55 Gy)
Parotid glands	Dmean ≤ 26 Gy
Oral cavity	Dmean 35–40 Gy
Brachial plexus	Dmax 65 Gy (D ₀₅ = 60 Gy)

Abbreviations: PTV = planning target volume; GTV = gross tumor volume; GTV_h = hypoxic GTV; CTV = clinical target volume; Dmax = dose to maximal point; Dmean = mean dose; D₉₅ = minimal dose to 95% of volume; D₀₅ = minimal dose to hottest 5% of volume.

Table 2

Comparison of average dose–volume histograms of clinically accepted IMRT plan and ¹⁸F-FMISO–guided IMRT plan

Structure	Clinically accepted IMRT plan/ ¹⁸ F-FMISO–guided IMRT plan			
	Dmax (Gy)	D ₀₅ (Gy)	D ₉₅ (Gy)	Dmean (Gy)
PTV _{p84}	—/92 ± 1	—/91 ± 2	—/84 ± 0.7	—/88 ± 1
PTV ₇₀	78 ± 2/91 ± 2	75 ± 2/81 ± 2	70 ± 2/70 ± 0.01	73 ± 1/75 ± 0.9
PTV _{59.4}	76 ± 2/82 ± 5	69 ± 4/72 ± 2	59 ± 2/59 ± 0.7	64 ± 1/65 ± 1
PTV ₅₄	66 ± 5/68 ± 8	60 ± 0.9/61 ± 2	54 ± 0.8/53 ± 1	57 ± 0.6/57 ± 1
Cord	44 ± 0.9/44 ± 1	41 ± 1/40 ± 2		30 ± 5/30 ± 4
Brain stem	48 ± 3/46 ± 4	42 ± 3/41 ± 3		20 ± 4 /19 ± 4
Left cochlea	40 ± 6/39 ± 8	37 ± 7/35 ± 7		29 ± 6/28 ± 7
Right cochlea	39 ± 8/38 ± 8	36 ± 7/34 ± 8		30 ± 7/29 ± 7
Left plexus	60 ± 3/62 ± 2	56 ± 2/58 ± 3		47 ± 8/49 ± 8
Right plexus	62 ± 3/63 ± 3	56 ± 2/57 ± 3		46 ± 7/48 ± 9
Left parotid	70 ± 6/71 ± 7	54 ± 7/54 ± 8		24 ± 2/24 ± 3
Right parotid	68 ± 9/68 ± 9	56 ± 10/55 ± 11		26 ± 2/25 ± 4
Oral cavity	67 ± 3/69 ± 3	58 ± 2/58 ± 3		37 ± 3/36 ± 2
Mandible	67 ± 4/69 ± 4	60 ± 4/60 ± 4		36 ± 6 /36 ± 6

Abbreviations: IMRT = intensity-modulate radiotherapy; ¹⁸F-FMISO = fluorine-18–labeled fluoromisonidazole; PTV₇₀ = 70 Gy delivered to PTV of clinically defined GTV; PTV_{p84} = 84 Gy delivered to GTV_h detected within primary GTV; PTV_{n84} = 84 Gy delivered to all GTV_h detected within all nodal GTVs; other abbreviations as in Table 1.

Note, GTV for hypoxia-guided plan excluded GTV_h.